Dan Ziegler,[1,2] Nikolaos Papanas,[1] Andrey Zhivov,[3] Stephan Allgeier,[4] Karsten Winter,[5] Iris Ziegler,[1] Jutta Brüggemann,[1] Alexander Strom,[1] Sabine Peschel,[3] Bernd Köhler,[6] Oliver Stachs,[3] Rudolf F. Guthoff,[3] and Michael Roden,[1,2] for the German Diabetes Study (GDS) Group*

Early Detection of Nerve Fiber Loss by Corneal Confocal Microscopy and Skin Biopsy in Recently Diagnosed Type 2 Diabetes

Diabetes 2014;63:2454–2463 | DOI: 10.2337/db13-1819

We sought to determine whether early nerve damage may be detected by corneal confocal microscopy (CCM), skin biopsy, and neurophysiological tests in 86 recently diagnosed type 2 diabetic patients compared with 48 control subjects. CCM analysis using novel algorithms to reconstruct nerve fiber images was performed for all fibers and major nerve fibers (MNF) only. Intraepidermal nerve fiber density (IENFD) was assessed in skin specimens. Neurophysiological measures included nerve conduction studies (NCS), quantitative sensory testing (QST), and cardiovascular autonomic function tests (AFTs). Compared with control subjects, diabetic patients exhibited significantly reduced corneal nerve fiber length (CNFL-MNF), fiber density (CNFD-MNF), branch density (CNBD-MNF), connecting points (CNCP), IENFD, NCS, QST, and AFTs. CNFD-MNF and IENFD were reduced below the 2.5th percentile in 21% and 14% of the diabetic patients, respectively. However, the vast majority of patients with abnormal CNFD showed concomitantly normal IENFD and vice versa. In conclusion, CCM and skin biopsy both detect nerve fiber loss in recently diagnosed type 2 diabetes, but largely in different patients, suggesting a patchy manifestation pattern of small fiber neuropathy. Concomitant NCS impairment points to an early parallel involvement of small and large fibers, but the precise temporal sequence should be clarified in prospective studies.

Diagnosis of diabetic sensorimotor polyneuropathy (DSPN) by clinical assessment may be variable even among proficient examiners and is less reproducible than usually assumed (1). Therefore, objective measures to accurately determine nerve pathology are required to detect early stages of DSPN, which may be more susceptible to intervention than late-stage sequelae. Small fibers, which constitute 70–90% of peripheral nerve fibers, may be quantified in skin biopsies by assessing intraepidermal nerve fiber density (IENFD), and it has been suggested that the earliest nerve fiber damage in DSPN is to the small fibers (2). Recently, corneal confocal microscopy (CCM), a noninvasive modality for the study of the human cornea, has emerged as a promising technique for the detection of small nerve fiber alterations (3,4).

CCM can be used to assess the corneal subbasal nerve plexus (SNP) lying between the basal epithelium and Bowman's membrane (5,6). Recent data suggest that CCM

[1]Institute for Clinical Diabetology, German Diabetes Center at Heinrich Heine University, Leibniz Center for Diabetes Research, Düsseldorf, Germany
[2]Department of Endocrinology and Diabetology, University Hospital, Düsseldorf, Germany
[3]Department of Ophthalmology, University of Rostock, Rostock, Germany
[4]Institute for Applied Computer Science and Automation, Karlsruhe Institute of Technology, Karlsruhe, Germany
[5]Translational Centre for Regenerative Medicine, University of Leipzig, Leipzig, Germany.
[6]Institute for Applied Computer Science, Karlsruhe Institute of Technology, Karlsruhe, Germany

Corresponding author: Dan Ziegler, dan.ziegler@ddz.uni-duesseldorf.de.

Received 29 November 2013 and accepted 23 February 2014.

This article contains Supplementary Data online at http://diabetes.diabetesjournals.org/lookup/suppl/doi:10.2337/db13-1819/-/DC1.

*The GDS Group consists of M. Roden (speaker), A. Buyken, J. Eckel, G. Giani, G. Geerling, H. Al-Hasani, C. Herder, A. Icks, J. Kotzka, O. Kuß, N. Marx, K. Müssig, B. Nowotny, P.J. Nowotny, W. Rathmann, J. Rosenbauer, P. Schadewaldt, N.C. Schloot, J. Szendroedi, and D. Ziegler.

See accompanying article, p. 2206.

shows good reproducibility (7) and could be useful to document nerve regeneration after treatment intensification and simultaneous pancreas and kidney transplantation (8,9). Previous works have also looked at its sensitivity and specificity for the diagnosis of DSPN (10,11), including comparison with IENFD (12). However, the vast majority of previous studies using CCM in diabetic patients have analyzed relatively small image frames of 0.15 mm^2, which may not be representative of larger corneal areas (13). As possible solutions, multiple nonoverlapping image frames per patient or larger mosaic images generated from image sequences have both been proposed (13,14). Moreover, image assessment has been hampered by the presence of ridge-like tissue deformations in the neighborhood of the SNP and image distortions. These are induced by the anterior corneal mosaic (ACM), which refers to a ridge and a groove pattern that can be induced on the epithelial surface and to an identical pattern seen deeper in the epithelium by retroillumination (15). Further progress has been accomplished with new technologies reconstructing SNP images from three-dimensional image stacks and generating an extended field of view by mosaicking these SNP images (15–17).

Peripheral nerve dysfunction may develop in patients with recently diagnosed diabetes (18,19) and even earlier in individuals with prediabetes (20,21). Whether CCM and skin biopsy may detect nerve pathology shortly after diagnosis of type 2 diabetes (T2D) and to what extent it correlates with measures of peripheral nerve function and structure is currently unknown. Therefore, the aim of this study was to evaluate the role of CCM compared with IENFD and quantitative small nerve fiber and large nerve fiber function tests in detecting early nerve damage in patients with recently diagnosed T2D.

RESEARCH DESIGN AND METHODS

The study was conducted in accordance with the Declaration of Helsinki and was approved by the ethics committee of Heinrich Heine University, Düsseldorf, Germany. All participants provided a written informed consent. Included were 86 patients with recently diagnosed T2D and 48 age- and sex-matched control subjects. Patients with diabetes were participants of the German Diabetes Study (GDS), which evaluates the long-term course of diabetes and its sequelae (ClinicalTrials.gov Identifier: NCT01055093) (18). Inclusion criteria for entry into the GDS are type 1 diabetes or T2D, known diabetes duration of $\leq$1 year, and age of 18–69 years at the baseline assessment. Exclusion criteria for the current study were secondary diabetes, pregnancy, severe diseases (cancer), psychiatric disorders, immunosuppressive therapy, limited cooperation ability, corneal disorders, and neuropathy from causes other than diabetes. Inclusion criteria for the control group were age of $\geq$18 years and a normal result on an oral glucose tolerance test (22), whereas exclusion criteria were neuropathy from any cause and those applied to the diabetic group. Among T2D subjects from the GDS who were asked to participate in the current study, ~50% agreed. Control subjects included staff from this institution and those recruited by newspaper advertisement.

CCM Examination

CCM was performed using a Heidelberg Retina Tomograph II (HRT II) with the Rostock Cornea Module (RCM; Heidelberg Engineering, Heidelberg, Germany), as previously described (15,16). The acquired images have a resolution of 384 × 384 pixels and the field of view is ~0.15 mm^2. Experienced ophthalmologists (A.Z. and S.P.) performed the examinations and were blinded to all study data, except for CCM and corneal sensation. The HRT II/RCM is equipped with a water contact objective (636/0.95 W, 670 nm; Zeiss, Jena, Germany). The distance from the cornea to the microscope was kept constant by a single-use contact element in sterile packaging (TomoCap). Coupling between the patient's cornea and the cap was facilitated with a thin lubricant layer of Vidisic gel (refractive index, 1.35; Bausch & Lomb/Dr. Mann Pharma, Berlin, Germany). The right eye was anesthetized by instilling Proparakain POS 0.5% eye drops (Ursapharm, Saarbrücken, Germany).

A modified, oscillating volume scan operating mode of the HRT II, in which the focus plane of the microscope is continually shifted back and forth, was used to acquire a number of image stacks (with an axial image distance of 0.5 μm) for each patient, with each stack representing a partial volume of the patient's cornea; particular care was taken that each image stack comprised the subbasal nerves over the entire height of present ACM ridges. A stack size of 96 images (scan depth, 48 μm) was chosen for ridge heights of less than 48 μm, and 120 images (60 μm) otherwise. At least three scans were performed for each patient, and the total duration of the microscopy was ~15 min.

All acquired image stacks were subsequently processed to correct motion artifacts, reconstruct the imaged volume, and compute a depth map of the SNP. An SNP image was composed for each image stack, and all reconstructed SNP images with common overlapping areas were combined into a mosaic image with an expanded field of view. Nerve structures and similar image features in the mosaic images were subsequently segmented. Wrongly segmented structures (reconstruction artifacts, dendritic cells, fibrotic tissue, etc.) were removed based on their morphological properties (size, elongation). In addition to the resulting image of the segmented nerve fibers, the network of fiber centerlines was finally calculated by thinning all segmented nerve fibers to a width of 1 pixel. A more detailed description is available in the Supplementary Data.

The segmentation image and the thinned fiber network image both formed the basis for the automated quantitative morphological and topological assessment of the

SNP (16,23). The following CCM parameters were determined: corneal nerve fiber (CNF) length (CNFL), defined as the total length of all nerve fibers (mm/mm^2); CNF density (CNFD), defined as the number of nerve fibers per mm^2; corneal nerve branch density (CNBD), defined as the number of branches per mm^2; average weighted CNF thickness (CNFTh), measured as mean thickness perpendicular to the nerve fiber course (μm); corneal nerve connecting points (CNCP), defined as the number of nerve fibers crossing area boundary (connections/mm); and average weighted CNF tortuosity (CNFTo), reflecting variability of nerve fiber directions and defined as total absolute nerve fiber curvature. Each fiber segment terminated by branching points, end points, and/or image borders was considered a distinct nerve fiber for the calculation of the above parameters. Weighting of single fibers was based on their contribution to the length of the total fiber network (15,16).

Morphometrical image analysis was performed for two different populations of segmented nerve fibers. Firstly, all CCM parameters were calculated for the whole fiber network. Thereafter, the determined lengths of all single nerve fiber segments were analyzed to identify an optimal length threshold at 93 μm that provided the most pronounced difference in CNFD between the diabetic and control groups. Finally, segmented nerve fibers shorter than this length threshold were removed, and a second set of CCM parameters was calculated for the remaining major nerve fibers (MNF) with length ≥93 μm only.

Corneal Sensation

Corneal esthesiometry was done using the Cochet-Bonnet esthesiometer (Luneau Ophthalmologie, Chartres, France). The nylon monofilament had a diameter of 0.12 mm and a fully extended length of 60 mm. The central, superior, inferior, nasal, and temporal cornea was touched once on each eye, beginning at a filament length of 60 mm. If a positive answer was not detected, the filament length was shortened in 5-mm steps each time and the procedure repeated until there was a positive response. Corneal sensation was calculated as the mean obtained from the five corneal areas on each eye.

Peripheral Nerve Function

Peripheral nerve function tests were performed as previously described (24). Motor nerve conduction velocity (NCV) was measured in the median, ulnar, and peroneal nerves, whereas sensory NCV and sensory nerve action potentials (SNAP) were determined in the median, ulnar, and sural nerves at a skin temperature of 33–34°C using surface electrodes (Nicolet VikingQuest; Natus Medical, San Carlos, CA). Quantitative sensory testing included measurement of the vibration perception threshold (VPT) at the second metacarpal bone and medial malleolus using the method of limits (Vibrameter; Somedic, Stockholm, Sweden) and thermal detection thresholds (TDT), including warm and cold thresholds at the thenar eminence and dorsum of the foot using the method of limits (TSA-II NeuroSensory Analyzer; Medoc, Ramat Yishai, Israel). Neurological examination was performed using the Neuropathy Disability Score (NDS) and Neuropathy Symptoms Score (NSS). Clinical DSPN was defined as NDS ≥6 and NSS ≥0, or NDS ≥3 and NSS ≥5 points (25). These and all other clinical examinations were performed by operators who were blinded to the corneal findings in all subjects.

IENFD

Three-millimeter skin punch biopsy specimens were taken under local anesthesia from the left lateral calf, ~10 cm proximal to the lateral malleolus. The tissue was fixed with 2% periodate-lysine-paraformaldehyde at 4°C for 24 h, rinsed twice for 10 min with 0.1 mol/L Sorensen buffer, and incubated in 33% sucrose for 3 h. After cryoprotection with 0.02 mol/L Sorensen buffer containing 20% glycerol at 4°C overnight, tissue was stored at −80°C.

Serial sections of skin specimens at 50-μm thickness were cut perpendicular to the skin surface at −20°C and −40°C, respectively. Staining of IENF was performed following the free-floating method as described before (26), with some modifications. In brief, sections were incubated after blocking with a rabbit anti-PGP9.5 antibody (1:1,200; Millipore, Temecula, CA) and a biotinylated anti-rabbit IgG antibody (1:100; Vector Laboratories, Burlingame, CA) for 1 h, followed by 1-h incubation with the Vector ABC kit and 3 min with the Vector SG substrate kit. All steps were performed at room temperature.

For the quantification of IENFD, a method adopted by the European Federation of Neurological Sciences (27) was used (28). Individual IENFs from four cross-sections per subject were visually counted along the length of the epidermis using a Leica DMRBE inverted microscope (Leica, Wetzlar, Germany) equipped with an Olympus DP73 digital color camera (Olympus, Hamburg, Germany). Only IENFs crossing the dermal-epidermal border were counted. The length of the epidermis was measured using cellSens 1.7 imaging software (Olympus Europa, Hamburg, Germany). IENFD was expressed as IENF/mm epidermis.

Cardiovascular Autonomic Function Tests

Cardiovascular autonomic nerve function was evaluated by measuring heart rate variability (HRV) during spontaneous breathing over 5 min (coefficient of R-R interval variation, spectral analysis), at deep breathing (expiration-to-inspiration ratio), after standing up (maximum-to-minimum 30:15 ratio), and in response to a Valsalva maneuver (Valsalva ratio) using VariaCardio TF5 (MIE Medical Research Ltd., Leeds, U.K.), as previously described (29).

Microvascular Complications and Physical Activity

Retinopathy was assessed by fundus photography using the panoramic ophthalmoscope P200C (Optos, Bruchsal, Germany) and diagnosed by an experienced ophthalmologist. Albuminuria was measured in 24-h urine samples

using a Cobas c 311 analyzer (Roche Diagnostics, Mannheim, Germany) and defined as normal (<20 μg/min), microalbuminuria (20–199 μg/min), and macroalbuminuria (≥200 μg/min). The level of physical activity was defined as low (<1 h/week over <1 month/year), moderate (1–2 h/week over 1–9 months/year), and high (>2 h/week over 9–12 months/year).

Statistical Analysis

Continuous data are expressed as mean ± SD. Categorical data were analyzed by Fisher exact test and are given as absolute or relative frequencies with 95% CI. For normally distributed data, parametric tests (*t* test or Pearson product-moment correlation), otherwise nonparametric tests (Mann-Whitney *U* test or Spearman rank correlation) were applied. To determine associations between two variables, univariate correlations and multiple linear regression analyses were performed. The level of significance was set at $\alpha = 0.05$.

RESULTS

The demographic and clinical characteristics of the patients and control subjects are reported in Table 1. Mean BMI and the percentage of clinical DSPN were higher in the diabetic group compared with the control subjects ($P < 0.05$). No significant differences between the groups were noted for sex, age, percentage of smokers, and systolic and diastolic blood pressure. The percentages of patients on diet-only, oral glucose–lowering drugs, and insulin were 39.5, 53.5, and 5.8%, respectively. Diabetes duration until CCM measurement was 2.1 ± 1.8 years. Laboratory parameters in the diabetic group included: HbA_{1c}, 6.8 ± 1.1% or 50.8 ± 12.0 mmol/mol; fasting blood glucose, 138 ± 37 mg/dL; fasting C-peptide, 3.3 ± 1.8 ng/mL; creatinine, 0.88 ± 0.17 mg/dL; triglycerides, 176 ± 100 mg/dL; total cholesterol, 212 ± 39 mg/dL; HDL cholesterol, 49 ± 12 mg/dL; and LDL cholesterol, 136 ± 36 mg/dL. Prevalence of microalbuminuria and macroalbuminuria was 15.1 and 3.5%, respectively, whereas nonproliferative (background) retinopathy was present in 2.3% of the patients. Treated hypertension was observed in 47.7% of the patients. The percentages of patients who were physically active to a moderate and high degree were 30.2 and 26.7%.

CCM measures, corneal sensation, IENFD, and peripheral and cardiovascular autonomic nerve function tests in the diabetic and control groups studied are presented in Table 2. Among the CCM measures, CNFL, CNFD, CNBD, CNCP, and CNFTh, and the corresponding MNF variables, were significantly reduced in the diabetic group compared with the control group (all $P < 0.05$), except for CNCP-MNF ($P = 0.107$). CNFTo-MNF tended to be higher in the diabetic group than in the control group ($P = 0.096$). No differences between the groups were found for CNFTh, CNFTh-MNF, and CNFTo. The CCM image area tended to be smaller in the diabetic group than in the control group ($P = 0.091$). Corneal sensation did not differ significantly between the groups. IENFD and median, ulnar, and peroneal motor NCV and median and sural sensory NCV and median, ulnar, and sural SNAP, cold TDT on the foot, expiration-to-inspiration ratio, and the Valsalva ratio were significantly lower, and metacarpal and malleolar VPT were significantly higher, in subjects with versus those without diabetes (all $P < 0.05$). No differences between the groups were noted for ulnar sensory NCV, warm and cold TDT on the thenar eminence, warm TDT on the foot, coefficient of R-R interval variation at rest, high-frequency and low-frequency power spectrum, and maximum-to-minimum 30:15 ratio.

Typical examples of CCM showing normal SNP appearance in a healthy subject and CNF loss in a patient with recently diagnosed T2D are shown in Fig. 1.

The percentages of values below the 2.5th percentile limit of normal were significantly higher for CNFL, CNFD-MNF, CNBD-MNF, IENFD, peroneal MNCV, sural SNCV, sural SNAP, and cold TDT, whereas the percentages of values above the 97.5th percentile were significantly higher for malleolar VPT and tended to be higher for warm TDT in subjects with T2D than in control subjects (Table 3). No significant differences between the groups were noted for the remaining parameters listed in Table 3. Only 2.7% (95% CI 0.5–8.4) of the patients had both abnormal CNFD and IENFD, whereas 65.8% (95% CI 55.6–74.9) had both normal CNFD and IENFD. Abnormal CNFD with concomitantly normal IENFD was noted in 20.5% (95% CI 13.1–29.9) of the diabetic group, whereas the opposite (i.e., normal

Table 1—Demographic and clinical characteristics of the diabetic and control groups studied

	Diabetic group *n* = 86	Control group *n* = 48	*P* value
Sex, % male	71	65	0.560
Age, years	57.6 ± 12.7	54.9 ± 12.7	0.251
BMI, kg/m^2	31.1 ± 5.7	25.2 ± 3.8	<0.001
Smoker, %	27	29	0.839
Blood pressure, mmHg			
Systolic	134 ± 15.9	131 ± 19.3	0.365
Diastolic	74.1 ± 9.0	74.8 ± 8.8	0.686
Clinical DSPN,* %	11.6 (6.4–18.9)	0	0.014

Data are shown as mean ± SD or as frequency (95% CI). *NDS ≥6 and NSS ≥0 or NDS ≥3 and NSS ≥5.

Table 2—Measures of CCM, corneal sensation, IENFD, and peripheral and cardiovascular autonomic nerve function in the diabetic and control groups studied

	Diabetic group (n = 86)	Control group (n = 48)	P value
CNFL (mm/mm^2)	19.7 ± 7.5	24.9 ± 6.5	<0.001
CNFL-MNF (mm/mm^2)	9.8 ± 3.6	11.9 ± 2.9	0.001
CNFD (n/mm^2)	299.2 ± 152.8	397.3 ± 165.3	0.001
CNFD-MNF (n/mm^2)	58.2 ± 23.4	73.1 ± 17.9	<0.001
CNBD (n/mm^2)	165.2 ± 96.4	226.7 ± 103.1	0.001
CNBD-MNF (n/mm^2)	68.8 ± 33.2	89.9 ± 26.3	<0.001
CNCP (n/mm)	6.84 ± 3.30	8.50 ± 3.25	0.006
CNCP-MNF (n/mm)	2.30 ± 1.43	2.71 ± 1.33	0.017
CNFTh (μm)	2.30 ± 0.06	2.31 ± 0.06	0.604
CNFTh-MNF (μm)	2.31 ± 0.07	2.31 ± 0.07	0.724
CNFTo	10.85 ± 4.04	9.83 ± 3.23	0.136
CNFTo-MNF	15.05 ± 3.98	13.89 ± 3.47	0.096
CCM image area (mm^2)	0.520 ± 0.281	0.603 ± 0.247	0.091
Corneal sensation right	5.95 ± 0.13	5.98 ± 0.06	0.074
Corneal sensation left	5.96 ± 0.12	5.98 ± 0.06	0.387
IENFD (n/mm)	8.3 ± 3.0	10.6 ± 3.6	<0.001
Median motor NCV (m/s)	52.4 ± 4.3	55.5 ± 3.8	<0.001
Ulnar motor NCV (m/s)	54.0 ± 5.6	58.2 ± 4.8	<0.001
Peroneal motor NCV (m/s)	42.6 ± 5.4	48.1 ± 4.5	<0.001
Median sensory NCV (m/s)	50.3 ± 6.9	54.5 ± 6.7	0.001
Median SNAP (μV)	4.81 ± 3.55	6.91 ± 4.34	0.004
Ulnar sensory NCV (m/s)	51.5 ± 5.6	52.8 ± 6.2	0.235
Ulnar SNAP (μV)	4.00 ± 2.48	5.86 ± 3.27	0.001
Sural sensory NCV (m/s)	42.0 ± 5.6	46.8 ± 4.1	<0.001
Sural SNAP (μV)	7.10 ± 5.04	9.77 ± 5.13	0.006
Metacarpal VPT (μm)	0.64 ± 0.56	0.34 ± 0.19	<0.001
Malleolar VPT (μm)	3.24 ± 4.35	1.10 ± 1.09	<0.001
Warm TDT thenar (°C)	34.2 ± 4.0	33.8 ± 0.7	0.477
Warm TDT foot (°C)	40.6 ± 4.4	39.8 ± 3.6	0.295
Cold TDT thenar (°C)	30.1 ± 1.2	30.4 ± 0.8	0.162
Cold TDT foot (°C)	26.1 ± 6.5	29.1 ± 1.8	<0.001
LF power spectrum (ms^2)	519 ± 1,276	706 ± 1,415	0.466
HF power spectrum (ms^2)	445 ± 1,185	639 ± 1,099	0.386
CV at rest (%)	4.36 ± 2.37	4.57 ± 2.45	0.666
CV during deep breathing (%)	6.45 ± 3.23	8.00 ± 3.14	0.013
Valsalva ratio	1.49 ± 0.26	1.64 ± 0.32	0.006

CV, coefficient of R-R interval variation; HF, high frequency; LF, low frequency.

CNFD and concomitantly abnormal IENFD) was found in 11.0% (95% CI 5.6–18.9) of the patients.

Correlation analysis in the control group showed no association between CCM measures and age, except for CNCP (r = −0.323; P = 0.025) and BMI. In the diabetic group, no correlation was observed between the CCM measures and IENFD (data not shown). The correlation analysis for the highest correlations ($r > 0.2$) for CCM measures with measures of peripheral nerve structure and function in the entire study population are reported in Table 4. The CCM measures correlated most consistently with median MNCV, median SNCV, and sural SNAP. IENFD correlated with each of the four CCM measures listed but was not associated with the CCM-MNF parameters. IENFD was correlated with each of the nerve conduction measures listed, except for ulnar SNCV.

DISCUSSION

In this study we demonstrate an early loss of small nerve fibers detected by both CCM and skin biopsy in recently

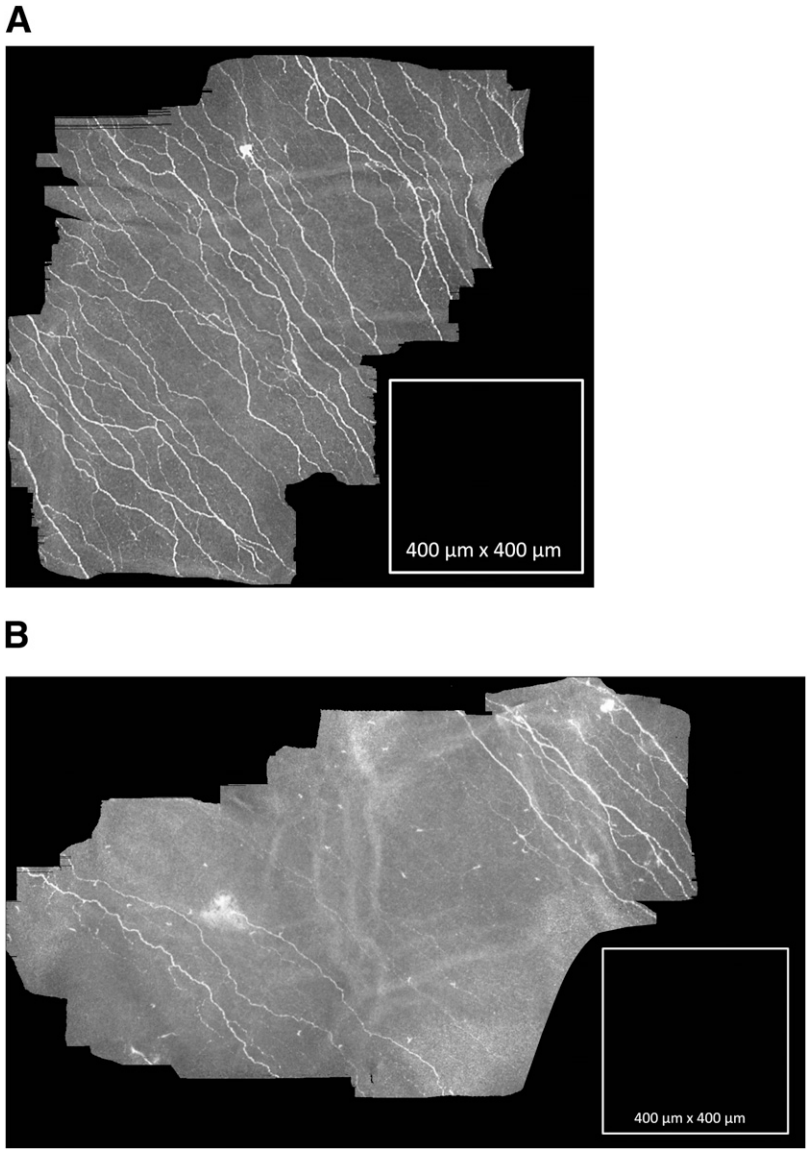

Figure 1—CCM showing the SNP. *A*: Normal SNP appearance in a healthy subject. *B*: CNF loss in a patient with recently diagnosed T2D. A single image frame with the commonly used size of 400 μm × 400 μm is displayed for comparison.

diagnosed T2D, with CNFD-MNF being most sensitive among six measures of CCM. However, these two techniques detect nerve pathologies largely in different groups of patients, suggesting a patchy manifestation pattern of small fiber neuropathy in various organs, possibly due to distinct underlying pathophysiological processes. Because nerve function assessed by nerve conduction studies (NCS), QST, and AFTs was also impaired, we suggest that a parallel involvement of small and large nerve fibers occurs in the early development of DSPN, but prospective studies are required to define the precise temporal sequence.

To the best of our knowledge, this is the first study reporting changes in the corneal SNP using CCM and IENFD using skin biopsy in recently diagnosed T2D. In the current study, the vast majority of the patients with abnormal CNFD showed concomitantly normal IENFD and vice versa. Consequently, small fiber pathology does not appear to develop simultaneously in different organs. This involvement of some but not other anatomical sites may be described as "patchy." However, it remains unclear why some patients develop a corneal neuropathy first, whereas in others, small fiber loss is first observed in the lower limbs. This finding should be further addressed in prospective studies.

Among the six CCM parameters assessed, CNFD-MNF emerged as the most sensitive in detecting corneal nerve pathology in 21% of the patients below the 2.5th percentile of the control group, followed by CNFL and CNBD-MNF with 17% each. This finding somewhat contrasts with a recent study reporting that among four CCM parameters, CNFL best discriminated DSPN case

Table 3—Percentages of CCM measures, IENFD, NCS, quantitative sensory testing, and cardiovascular autonomic nerve function tests below the 2.5th or above the 97.5th percentile limit of normal in the diabetic and control groups studied

	Diabetic group, % (95% CI)	Control group, % (95% CI)	*P* value
CNFL	18.6 (12.0–26.9)	4.2 (0.8–12.5)	0.019
CNFL-MNF	17.4 (11.1–25.6)	6.3 (1.7–15.4)	0.111
CNFD	5.8 (2.3–11.8)	0	0.160
CNFD-MNF	20.9 (14.0–29.4)	6.3 (1.7–15.4)	0.027
CNBD	4.7 (1.6–10.3)	0	0.296
CNBD-MNF	17.4 (11.1–25.6)	4.2 (0.8–12.5)	0.031
CNCP	4.7 (1.6–10.3)	0	0.296
CNCP-MNF	0	0	—
IENFD	13.7 (7.6–22.1)	0	0.013
Peroneal motor NCV	31.4 (23.2–40.6)	2.3 (0.1–10.6)	<0.001
Sural sensory NCV	35.7 (27.0–45.2)	0	<0.001
Sural SNAP	24.1 (16.6–33.1)	0	<0.001
Malleolar VPT	30.6 (22.4–39.8)	0	<0.001
Warm TDT foot	9.3 (4.7–16.2)	0	0.052
Cold TDT foot	26.7 (19.0–35.7)	2.4 (0.1–10.8)	0.001
CV at rest	14.3 (8.2–22.5)	10.0 (3.5–21.4)	0.575
CV during deep breathing	14.3 (8.2–22.5)	4.9 (0.9–14.6)	0.215

CV, coefficient of R-R interval variation.

patients from control subjects (11). It also contrasts with a previous report that demonstrated a significant reduction in CNFD and CNBD but not CNFL in several groups of diabetic patients with mild to severe DSPN with a mean diabetes duration between 18.4 and 25.2 years and no reduction in CNFL and CNFD in patients without clinical DSPN who had diabetes for 16.7 years on average (12). Furthermore, we found no correlation between CCM measures and AFTs, in contrast to a recent study showing that CNFL, CNFD, and CNBD correlated with HRV during deep breathing in patients with type 1 diabetes and an average diabetes duration of 22.5 years (30). The reasons for these discrepancies could be due to the differences in study populations, CCM equipment, the size of the corneal area, and the image-processing software algorithms used.

The CCM examination process used in this study is fundamentally based on highly adapted software, comprising a modified version of the microscope control software (oscillating volume scan operating mode) and the entirety of the custom-made image processing algorithms used thereafter, including motion correction, volume reconstruction, SNP layer extraction, mosaicking, segmentation of the subbasal nerve fibers, and quantitative

Table 4—Correlation coefficients (*r*) for the relationships between measures of CCM, IENFD, and NCS in the entire study population (*N* = 134)

	MNCV			SNCV			SNAP	
	Median	Ulnar	Peroneal	Median	Ulnar	Sural	Sural	IENFD
CNFL	0.327*	0.158	0.152	0.252*	0.122	0.119	0.260*	0.219*
CNFL-MNF	0.249*	0.194*	0.166	0.219*	0.160	0.142	0.226*	0.117
CNFD	0.298*	0.096	0.111	0.201*	0.051	0.085	0.221*	0.204*
CNFD-MNF	0.281*	0.189*	0.182*	0.248*	0.178*	0.136	0.255*	0.108
CNBD	0.299*	0.101	0.122	0.216*	0.051	0.081	0.222*	0.184*
CNBD-MNF	0.295*	0.160	0.145	0.244*	0.131	0.123	0.288*	0.133
CNCP	0.268*	0.231*	0.144	0.192*	0.207*	0.182*	0.203*	0.262*
CNCP-MNF	0.192*	0.189*	0.130	0.099	0.212*	0.123	0.130	−0.025
IENFD	0.278*	0.421*	0.278*	0.220*	0.100	0.314*	0.196*	—

*$P < 0.05$.

morphometric assessment. This approach enabled us to robustly generate and analyze images of the SNP layer with an extended field of view and devoid of ACM-induced artifacts (15–17). The entire process also features a higher degree of automation than would have been achievable by using standard image-processing software.

It currently remains an open question whether our approach actually yields a better diagnostic value than recording and examining a small set of CCM images (4,7,10,12,13), the technique most commonly used by other CCM research groups, and if it does, whether the differences are significant enough to justify the higher effort in examination time. Such comparative studies are presently being conducted.

We used a two-step CCM image analysis, the first for the entire fiber network and the second for MNF only. This approach provides a more detailed insight into the morphological and topological structure of the segmented nerve fibers. Our data indicate that the use of a threshold based on fiber length could be useful to improve the discriminatory power of CNFD and CNBD. Furthermore, this strategy allows a comparison of data generated for research purposes with those used for diagnostic reasons. Comprehensive image processing–oriented approaches aim at the best possible and preferably complete detection of nerve fibers. This includes total elimination of all image artifacts and segmentation even of the faintest fibers. On the other hand, for clinical purposes, identification of MNF to obtain CNFD and CNBD may be sufficient.

Previous studies have shown correlations of CCM measures with VPT (31), clinical severity of DSPN (4,10,12,32,33), NCS (12,32), HRV (12,30), cold TDT (12,30), and IENFD (12) in longer-standing diabetes. In the current study, several CCM measures correlated with IENFD and with median and ulnar motor and sensory NCV, as well as sural SNAP, in the entire study population, but the relationship was modest to moderate. This is in line with the aforementioned studies (12,32,34) supporting the notion that the pathophysiology underlying the manifestation of neuropathy in the cornea may be different from DSPN affecting the lower limbs. Indeed, vascular factors including reduced endoneurial blood flow and microvascular alterations appear to contribute to the pathogenesis of DSPN (35,36), whereas the normal cornea, albeit being the most densely innervated tissue in the human body (several 100-fold higher than skin) (37), is devoid of blood vessels. However, many corneal abnormalities may disrupt the avascular microenvironment and lead to corneal angiogenesis. Recent experimental evidence suggests that sensory nerves and neovessels inhibit each other in the cornea. When vessel growth is stimulated, nerves disappear, and conversely, denervation induces angiogenesis (38). Hence, whereas angiogenesis may be a consequence of corneal denervation, neuropathy in the lower limbs may be a consequence of reduced angiogenesis and may be treated by promoting angiogenesis (39). Thus, on one hand, in view of this distinct pathophysiological background, the lack of close correlations between measures of CCM and peripheral nerve tests may not be surprising. On the other hand, advanced glycation end-product immunoreactivity was observed in epithelial cells, epithelial basement membrane, and stromal keratocytes in corneas from diabetic monkeys (40), suggesting that one possible mechanism for the development of corneal neuropathy could be nonenzymatic glycation, similar to its putative role in the pathogenesis of DSPN (36).

The relatively high prevalence of micro/macroalbuminuria (18.6%) compared with retinopathy (2.3%) may be explained by the high percentage of treated hypertension (48%). These findings are compatible with those reported by the Hoorn study in newly diagnosed T2D subjects (41).

The strengths of this work are the inclusion of a relatively large and homogenous study population with recently diagnosed T2D, the use of novel image-processing algorithms to reconstruct SNP images with an extended field of view from three-dimensional image stacks, and the detailed quantitative assessment of neuropathy, including skin biopsy, to detect small fiber neuropathy.

A limitation is the cross-sectional nature of this study so that the predictive value and further course of the described corneal and intraepidermal nerve damage cannot be determined at present. The precise temporal sequence of alterations to small versus large nerve fibers can only be established in prospective studies. Moreover, our approach to compare the value of counting all CNFs with counting MNF only to detect abnormality may be biased toward a better outcome for MNF and is only valid in the present population. Finally, selection bias cannot be excluded, because the patients and control subjects included in this study may not be representative of the general population.

The clinical implications of the current study may be outlined as follows. In recently diagnosed T2D, CCM may be used to detect early evidence of neuropathy in the cornea. The CCM examination could be useful for timely diagnosis, because IENFD may be normal in some patients with CCM abnormalities. However, before CCM can be recommended for use in clinical practice, further validation determining its value in predicting DSPN and its susceptibility to interventions is required.

In conclusion, we have demonstrated corneal nerve pathology in recently diagnosed T2D. In this setting, CCM detects early nerve fiber loss slightly more frequently than a skin biopsy, but not necessarily in the same patients, suggesting a patchy manifestation pattern of small fiber neuropathy. In some patients, CNF loss may even be the first evidence of subclinical DSPN. These results indicate that CCM could be established as a powerful noninvasive tool for an early detection of neuropathy, but prospective studies are required to confirm this notion.

Acknowledgments. The authors thank the staff of the GDS, especially M. Behler and M. Schroers-Teuber, for their excellent technical support.

Funding. The GDS was initiated and financed by the German Diabetes Center, which is funded by the German Federal Ministry of Health (Berlin, Germany), the Ministry of Innovation, Science, Research and Technology of the state North Rhine-Westphalia (Düsseldorf, Germany), and grants from the German Federal Ministry of Education and Research (BMBF) to the German Center for Diabetes Research (DZD e.V.). Parts of this work were supported by a grant from the Ministry of Science, Research and the Arts of Baden-Württemberg (AZ 33-7533-7-11.6-9/3/1).

Duality of Interest. No potential conflicts of interest relevant to this article were reported.

Author Contributions. D.Z. designed the study. D.Z., N.P., A.Z., S.A., K.W., I.Z., J.B., A.S., S.P., B.K., and O.S. researched data. D.Z. and N.P. wrote the manuscript. R.F.G. and M.R. contributed to discussion. D.Z., N.P., A.Z., S.A., K.W., I.Z., J.B., A.S., S.P., B.K., O.S., R.F.G., and M.R. reviewed and edited the manuscript. D.Z. is the guarantor of this work and, as such, had full access to all of the data in the study and takes responsibility for the integrity of the data and the accuracy of the data analysis.

References

1. Dyck PJ, Albers JW, Andersen H, et al.; on behalf of the Toronto Expert Panel on Diabetic Neuropathy. Diabetic polyneuropathies: update on research definition, diagnostic criteria and estimation of severity. Diabetes Metab Res Rev 2011;27:620–628

2. Malik R, Veves A, Tesfaye S, et al.; on behalf of the Toronto Consensus Panel on Diabetic Neuropathy. Small fiber neuropathy: role in the diagnosis of diabetic sensorimotor polyneuropathy. Diabetes Metab Res Rev 2011;27:678–684

3. Rosenberg ME, Tervo TM, Immonen IJ, Müller LJ, Grönhagen-Riska C, Vesaluoma MH. Corneal structure and sensitivity in type 1 diabetes mellitus. Invest Ophthalmol Vis Sci 2000;41:2915–2921

4. Malik RA, Kallinikos P, Abbott CA, et al. Corneal confocal microscopy: a non-invasive surrogate of nerve fibre damage and repair in diabetic patients. Diabetologia 2003;46:683–688

5. Zhivov A, Blum M, Guthoff R, Stachs O. Real-time mapping of the subepithelial nerve plexus by in vivo confocal laser scanning microscopy. Br J Ophthalmol 2010;94:1133–1135

6. Papanas N, Ziegler D. Corneal confocal microscopy: a new technique for early detection of diabetic neuropathy. Curr Diab Rep 2013;13:488–499

7. Hertz P, Bril V, Orszag A, et al. Reproducibility of in vivo corneal confocal microscopy as a novel screening test for early diabetic sensorimotor polyneuropathy. Diabet Med 2011;28:1253–1260

8. Tavakoli M, Kallinikos P, Iqbal A, et al. Corneal confocal microscopy detects improvement in corneal nerve morphology with an improvement in risk factors for diabetic neuropathy. Diabet Med 2011;28:1261–1267

9. Tavakoli M, Mitu-Pretorian M, Petropoulos IN, et al. Corneal confocal microscopy detects early nerve regeneration in diabetic neuropathy after simultaneous pancreas and kidney transplantation. Diabetes 2013;62:254–260

10. Tavakoli M, Quattrini C, Abbott C, et al. Corneal confocal microscopy: a novel noninvasive test to diagnose and stratify the severity of human diabetic neuropathy. Diabetes Care 2010;33:1792–1797

11. Ahmed A, Bril V, Orszag A, et al. Detection of diabetic sensorimotor polyneuropathy by corneal confocal microscopy in type 1 diabetes: a concurrent validity study. Diabetes Care 2012;35:821–828

12. Quattrini C, Tavakoli M, Jeziorska M, et al. Surrogate markers of small fiber damage in human diabetic neuropathy. Diabetes 2007;56:2148–2154

13. Vagenas D, Pritchard N, Edwards K, et al. Optimal image sample size for corneal nerve morphometry. Optom Vis Sci 2012;89:812–817

14. Turuwhenua JT, Patel DV, McGhee CN. Fully automated montaging of laser scanning in vivo confocal microscopy images of the human corneal subbasal nerve plexus. Invest Ophthalmol Vis Sci 2012;53:2235–2242

15. Allgeier S, Zhivov A, Eberle F, et al. Image reconstruction of the subbasal nerve plexus with in vivo confocal microscopy. Invest Ophthalmol Vis Sci 2011;52:5022–5028

16. Zhivov A, Winter K, Hovakimyan M, et al. Imaging and quantification of subbasal nerve plexus in healthy volunteers and diabetic patients with or without retinopathy. PLoS ONE 2013;8:e52157

17. Köhler B, Allgeier S, Eberle F, et al. [Image reconstruction of the corneal subbasal nerve plexus with extended field of view from focus image stacks of a confocal laser scanning microscope]. Klin Monatsbl Augenheilkd 2011;228:1060–1066

18. Ziegler D, Papanas N, Roden M; GDC Study Group. Neuropad: evaluation of three cut-off points of sudomotor dysfunction for early detection of polyneuropathy in recently diagnosed diabetes. Diabet Med 2011;28:1412–1415

19. Ziegler D, Mayer P, Gries FA. Evaluation of thermal, pain, and vibration sensation thresholds in newly diagnosed type 1 diabetic patients. J Neurol Neurosurg Psychiatry 1988;51:1420–1424

20. Papanas N, Vinik AI, Ziegler D. Neuropathy in prediabetes: does the clock start ticking early? Nat Rev Endocrinol 2011;7:682–690

21. Bongaerts BW, Rathmann W, Kowall B, et al. Postchallenge hyperglycemia is positively associated with diabetic polyneuropathy: the KORA F4 study. Diabetes Care 2012;35:1891–1893

22. American Diabetes Association. Diagnosis and classification of diabetes mellitus. Diabetes Care 2012;35(Suppl. 1):S64–S71

23. Winter K, Zhivov A, Guthoff RF, Köhler B, Stachs O. Characteristic quantities for the quantification of CLSM images of the subbasal nerve plexus. Biomed Tech (Berl) 2010;55(Suppl. 1):252–254

24. Ziegler D, Siekierka-Kleiser E, Meyer B, Schweers M. Validation of a novel screening device (NeuroQuick) for quantitative assessment of small nerve fiber dysfunction as an early feature of diabetic polyneuropathy. Diabetes Care 2005;28:1169–1174

25. Young MJ, Boulton AJ, MacLeod AF, Williams DR, Sonksen PH. A multicentre study of the prevalence of diabetic peripheral neuropathy in the United Kingdom hospital clinic population. Diabetologia 1993;36:150–154

26. McCarthy BG, Hsieh ST, Stocks A, et al. Cutaneous innervation in sensory neuropathies: evaluation by skin biopsy. Neurology 1995;45:1848–1855

27. Lauria G, Cornblath DR, Johansson O, et al.; European Federation of Neurological Societies. EFNS guidelines on the use of skin biopsy in the diagnosis of peripheral neuropathy. Eur J Neurol 2005;12:747–758

28. Lauria G, Bakkers M, Schmitz C, et al. Intraepidermal nerve fiber density at the distal leg: a worldwide normative reference study. J Peripher Nerv Syst 2010;15:202–207

29. Ziegler D, Laux G, Dannehl K, et al. Assessment of cardiovascular autonomic function: age-related normal ranges and reproducibility of spectral analysis, vector analysis, and standard tests of heart rate variation and blood pressure responses. Diabet Med 1992;9:166–175

30. Sivaskandarajah GA, Halpern EM, Lovblom LE, et al. Structure-function relationship between corneal nerves and conventional small-fiber tests in type 1 diabetes. Diabetes Care 2013;36:2748–2755

31. Messmer EM, Schmid-Tannwald C, Zapp D, Kampik A. In vivo confocal microscopy of corneal small fiber damage in diabetes mellitus. Graefes Arch Clin Exp Ophthalmol 2010;248:1307–1312

32. Nitoda E, Kallinikos P, Pallikaris A, et al. Correlation of diabetic retinopathy and corneal neuropathy using confocal microscopy. Curr Eye Res 2012;37:898–906

33. Petropoulos IN, Alam U, Fadavi H, et al. Corneal nerve loss detected with corneal confocal microscopy is symmetrical and related to the severity of diabetic polyneuropathy. Diabetes Care 2013;36:3646–3651

34. Edwards K, Pritchard N, Vagenas D, Russell A, Malik RA, Efron N. Utility of corneal confocal microscopy for assessing mild diabetic neuropathy: baseline findings of the LANDMark study. Clin Exp Optom 2012;95:348–354

35. Quattrini C, Jeziorska M, Boulton AJ, Malik RA. Reduced vascular endothelial growth factor expression and intra-epidermal nerve fiber loss in human diabetic neuropathy. Diabetes Care 2008;31:140–145
36. Sytze Van Dam P, Cotter MA, Bravenboer B, Cameron NE. Pathogenesis of diabetic neuropathy: focus on neurovascular mechanisms. Eur J Pharmacol 2013;719:180–186
37. Bonini S, Rama P, Olzi D, Lambiase A. Neurotrophic keratitis. Eye (Lond) 2003;17:989–995
38. Ferrari G, Hajrasouliha AR, Sadrai Z, Ueno H, Chauhan SK, Dana R. Nerves and neovessels inhibit each other in the cornea. Invest Ophthalmol Vis Sci 2013; 54:813–820
39. Ropper AH, Gorson KC, Gooch CL, et al. Vascular endothelial growth factor gene transfer for diabetic polyneuropathy: a randomized, double-blinded trial. Ann Neurol 2009;65:386–393
40. Zou C, Wang S, Huang F, Zhang YA. Advanced glycation end products and ultrastructural changes in corneas of long-term streptozotocin-induced diabetic monkeys. Cornea 2012;31:1455–1459
41. Spijkerman AM, Dekker JM, Nijpels G, et al. Microvascular complications at time of diagnosis of type 2 diabetes are similar among diabetic patients detected by targeted screening and patients newly diagnosed in general practice: the Hoorn screening study. Diabetes Care 2003;26:2604–2608